City Research Online

City St George's, University of London

Citation: Tajudin, M. F. M., Ahmad, A. H., Alias, J., Maarof, M. R. & Naher, S. (2026). Application of Response Surface Methodology for Optimizing Direct Thermal Method Parameters of Al-Si Alloys with Mg Addition. Journal of Materials Engineering and Performance, doi: 10.1007/s11665-026-13905-z

This is the accepted version of the paper.

This version of the publication may differ from the final published version. To cite this item please consult the publisher's version.

Permanent repository link: https://openaccess.city.ac.uk/id/eprint/37574/

Link to published version: https://doi.org/10.1007/s11665-026-13905-z

Copyright and Reuse: Copyright and Moral Rights remain with the author(s) and/or copyright holders. Copies of full items can be used for personal research or study, educational, or not-for-profit purposes without prior permission or charge, unless otherwise indicated, provided that the authors, title and full bibliographic details are credited, a hyperlink and/or URL is given for the original metadata page and the content is not changed in any way. For full details of reuse please refer to City Research Online policy.

City Research Online: http://openaccess.city.ac.uk/ publications@citystgeorges.ac.uk

Application of Response Surface Methodology for Optimizing Direct Thermal Method Parameters of Al-Si Alloys with Mg Addition

M. F. M. Tajudin[1], *A. H. Ahmad[1,2], J. Alias[1,2], M. R. Maarof[1], S. Naher[3]

[1]*Faculty of Mechanical and Automotive Engineering Technology, Universiti Malaysia Pahang Al-Sultan Abdullah, 26600 Pekan, Pahang, Malaysia*
[2]*Centre for Automotive Engineering, Universiti Malaysia Pahang Al-Sultan Abdullah, 26600 Pekan, Pahang, Malaysia.*
[3]*Department of Mechanical Engineering and Aeronautics, City University of London, London EC1V 0HB, UK.*

**asnul@umpsa.edu.my*

Abstract

This study examines the effects of varying processing parameters, including pouring temperature (590 °C, 610 °C, 630 °C), holding time (10 s, 15 s, 20 s), and magnesium addition (0.5 wt.%, 1 wt.%, 1.5 wt.%), on the material. The semi-solid feedstock billets were produced using the Direct Thermal Method (DTM). Additionally, an extra sample with a pouring temperature of 590 °C and a holding time of 20 s was produced without magnesium addition to serve as a reference. The samples underwent mechanical testing, including density measurement, tensile, and Vickers hardness tests. The results showed that sample 7, with a pouring temperature of 590 °C, a holding time of 15 s, and a magnesium addition of 1.5 wt.%, has the highest density value, UTS, YS, and Vickers hardness value at 2.7 g/cm^{3,} 147 MPa, 113 MPa, and 137 HV. Meanwhile, sample 16 without magnesium addition has the lowest density and mechanical properties, with a density, UTS, YS, and Vickers hardness value of 2.53 g/cm^3, 44 MPa, 36 MPa, and 73 HV, respectively. It was apparent that the sample with magnesium addition had better mechanical properties than those without magnesium addition. The samples exhibited dimple cracks, demonstrating the alloys' ductile fracture characteristic. RSM has explored the optimal combination of pouring temperature, holding time, and magnesium addition to produce Al-Si alloy semi-solid feedstock billets with the desired mechanical properties, as produced via DTM. Experimental and predicted values show a good level of agreement. The experimental findings elucidate the impact of magnesium addition on the mechanical characteristics of the Al-Si alloy, which is well-suited for SSM processing.

Keywords: Lightweight structural materials; Semi-solid metal processing; Aluminium silicon alloy; Direct thermal method; Grain refinement; Mechanical properties; statistical optimization.

1. Introduction

A growing need for lightweight, fuel-efficient, and environmentally friendly vehicles has led to an accelerated shift in the materials used in the automotive and transportation sectors. In particular, the rise of electric and hybrid vehicles has intensified the demand for lightweight structural materials that meet severe performance requirements [1], [2]. This shift reflects the critical need to reduce energy consumption while maintaining and enhancing the mechanical properties of automotive components. Consequently, the production of high-quality aluminium alloy components is becoming increasingly urgent. Nevertheless, intensive research is underway to fully exploit the potential of aluminium used in various manufacturing sectors. In recent decades, aluminium alloys have

become increasingly popular in construction due to their advantageous properties surpassing those of traditional steel components [1], [3], [4], [5]. This has led to a surge in research to better understand their structural behavior and develop design principles. Aluminium alloy is widely recognised across multiple sectors for its exceptional qualities, including corrosion resistance, lightweight construction, high strength, remarkable resistance to low temperatures, and simplicity of extrusion moulding.

However, the aluminium casting industry continues to encounter problems, particularly in the demand for new types of aluminium products with exceptional performance that are produced using more efficient processes. The use of aluminium alloy continues to evolve due to the limitations of the conventional casting process, which is associated with numerous defects such as shrinkage, porosity, and hot cracking as well as growing demand for improved access to predictive and actual product performance testing facilities [6], [7], [8]. Consequently, the semi-solid metal (SSM) processing, which Fleming discovered in the 1970s, was one of the most momentous and consequential of that decade [9], [10], [11]. The SSM processing technique was subjected to the material's behaviour in semi-solid-state conditions.

The SSM processing is a manufacturing technique in which an alloy is injected into a die as a slurry containing nearly spherical primary particles suspended in a liquid matrix. SSM processing has been widely used in the automotive industry, as it produces near-net-shape components with better dimensional tolerances, good surface quality, reduced porosity, and rapid output [1], [12], [13]. The microstructural behaviours of the SSM processing were characterised by a liquid-like flow behaviour when shear was applied, and solid-like behaviour was observed under rest conditions. The microstructure formation of the SSM processing must contain a near-globular grain structure that is encompassed by the liquid matrix, with a wide transition area between the solidus and liquidus temperatures. The experiment conducted by Fleming and his colleagues revealed that the microstructure of Sn-Pb15 alloy was strongly affected by the constant shearing forces applied to the alloy while it was in the semi-solid state [14]. Specifically, the study demonstrated that the shearing action leads to the development of a globular grain structure [10, 15], a characteristic of SSM processing alloys, as shown in Figure 1.

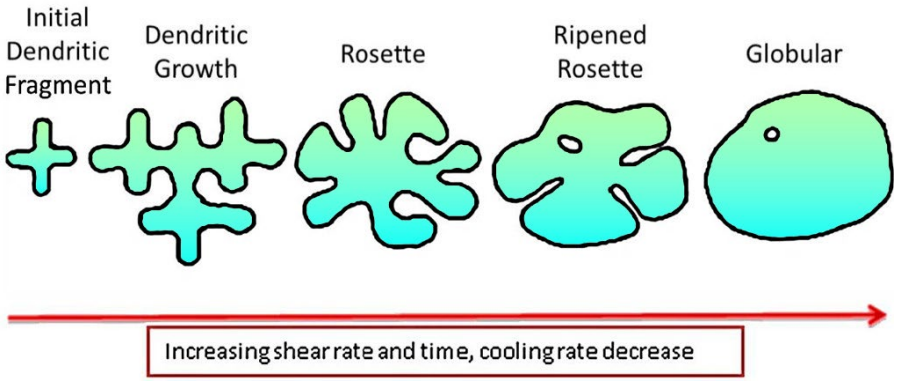

Figure 1: Evolution of the primary phase during the solidification process [15].

Various processing methods have been developed recently to produce globular grain structures within the SSM processing. Despite all methods capable of generating feedstock billets with globular grain structure, the Direct

Thermal Method (DTM) stands out as a preferred option due to its simplicity, low equipment requirements, and low processing costs [16], [17], [18], [19]. In this approach, the low superheat alloy is poured into a cylindrical copper mould, whose high thermal conductivity facilitates rapid heat extraction and promotes the formation of a globular microstructure [17], [20], [21]. Numerous studies have demonstrated that the processing parameters, particularly pouring temperature and holding time, critically influence the evolution of the microstructure during solidification [22], [23], [24], [25].

The implementation of experimental design as a robust statistical instrument facilitates the modification of process variability while simultaneously addressing the requirement for diminished resources. Response Surface Methodology (RSM) is a statistical modelling instrument and mathematical technique that facilitates the relation between independent variables and one or more response, while optimising the conditions to achieve maximum efficiency with reduced unnecessary cost and time [26], [27], [28]. The RSM approach is based on the fit of mathematical models including linear, quadratic polynomial functions and others to the experimental outcomes derived from the designed experiments, as well as the validation of the model obtain through statistical techniques. The design of experiment (DOE) is a fundamental instrument in engineering field where this technique is particularly useful for enhancing the efficiency of process [26]. The fundamental objective of DOE is to vary all crucial parameters simultaneously over a range of designed experiments and subsequently to integrate the findings via a mathematical model. Then, this mathematical model can be used for optimisation and prediction. This improvement results in enhanced process performance, a decrease in the number of variables and consequently lower operational cost and reduced experimental time [26].

Mechanical properties are among the most fundamental principles in developing well-designed components across various industries. The growing provision of better mechanical properties in aluminium alloys has become essential in producing high-strength and ductile aluminium alloys [29]. Grain refinement is a method for enhancing the mechanical properties of alloys, reducing grain size, and promoting a more uniform microstructure [30]. Controlling grain size is critical for achieving superior mechanical properties in cast and wrought aluminium alloys [31]. Granger et al. [31] found that the mechanical properties of structural components suffer a significant decline when a uniform grain size distribution is not achieved. Magnesium (Mg) is a common alloying element used in Al-Si-Cu casting alloys to improve their mechanical characteristics [32]. Throughout the solidification process, intermetallic phases formed under different conditions collectively contributed to the material's performance [33], [34], [35]. Furthermore, the morphology of the Mg_2Si phase can be modified and improved throughout the SSM process using lower pouring temperatures than those of the conventional casting method.

Although the impact of adding Mg to conventionally cast aluminium silicon alloys has been thoroughly studied, there is limited information and a lack of intensive research on the effect of Mg addition on the semi-solid mechanical properties of cast aluminium alloy, particularly when manufactured via the Direct Thermal Method (DTM). This data is crucial in SSM processing research and plays a pivotal role in determining suitable processing parameters for manufacturing. Therefore, conducting comprehensive experimental studies is imperative to gain deeper insights into the properties of cast Al-Si alloy with Mg addition as a semi-solid metal billet feedstock.

2. Experimental procedure

As-cast aluminium silicon (Al-Si) alloy was used in this experimental work. The Optical Emission Spectroscopy (OES) was calibrated before being used to determine the chemical composition of the as-received material. Three chemical compositions were carried out to obtain accurate results. Table 1 presents the chemical composition of the as-received material of the Al-Si alloy.

Table 1: Chemical composition of aluminium alloy used in this experimental work.

Element	Si	Zn	Cu	Fe	Ni	Mn	Mg	Cr	Ti	Al
Composition (wt%)	9.76	1.48	1.16	0.69	0.54	0.31	0.23	0.11	0.09	Balance

2.1 Box-Behnken Experimental Design & Response Surface Methodology

The experimental conditions adhered to a response surface methodology (RSM) incorporating a Box-Behnken Design with 3 factors at 3 levels, set at equidistant values (-1, 0, 1). The BBD accurately describes the linear, quadratic and interaction effects as a second-order polynomial used in the modelling. Analysis of Variance (ANOVA) and the RSM were carried out using Design-Expert software, which is version 13. The first-order model was employed for the linear relationship between the independent variables as in Eq 1.

$$Y = \beta_0 + \beta_i X_i + \beta_{ii} X_{ii} + X_i X_j \quad \text{Eq 1}$$

The second-order polynomial model utilised in the response surface analysis was described by the following Eq 2.

$$Y = \beta_0 + \Sigma_{i=1}^{k} \beta_i X_i + \Sigma_{i=1}^{k} \beta_{ii} X_i^2 + \Sigma_{i<1}^{k} \Sigma \beta_{ij} X_i X_j \quad \text{Eq 2}$$

Where Y is the predicted response value, β_0 is a constant, β_i is a constant, β_{ii} is the quadratic coefficient, and $\beta_{ij}$is the interaction coefficient. Meanwhile, X_i and X_j are the independent variables. The BBD of Design of Experiment (DOE) software was used to design the experimental parameters for the study. The BBD method incorporates three factors: pouring temperature X_1, holding time X_2, and magnesium addition X_3. A total of 15 DTM feedstock billets were produced using the BBD design, with an additional sample produced without magnesium addition to serve as a reference. This control sample enabled a more precise comparison and better understanding of the effect of magnesium addition on the mechanical properties of DTM feedstock billets. The processing parameters used in the experimental study were obtained from thermal analysis experiments [36]. Table 2 represents the levels and ranges of the selected independent variables. Table 3 represents the RSM experimental design using the BBD method.

Table 2: Levels, factors, and experimental independent variables for DTM using the BBD method.

Factors	Independent Variables	Units	Symbol	Code Values		
				-1	0	1
A	Pouring Temperatures	ºC	X_1	590	610	630
B	Holding Time	s	X_2	10	15	20
C	Magnesium Addition	Wt.%	X_3	0.5	1	1.5

Table 3: A design expert using the BBD method generated the processing parameters used in this experimental work.

Run	X_1: Pouring temperature (°C)	X_2: Holding time (s)	X_3: Magnesium addition (wt.%)
1	590	10	1
2	630	10	1
3	590	20	1
4	630	20	1
5	590	15	0.5
6	630	15	0.5
7	590	15	1.5
8	630	15	1.5
9	610	10	0.5
10	610	20	0.5
11	610	10	1.5
12	610	20	1.5
13	610	15	1
14	610	15	1
15	610	15	1
16	590	20	-

2.2 Direct Thermal Method (DTM) Experiment Procedure

The experimental procedure used in this study closely follows the DTM previously detailed in our earlier publication [37], [38]. Only modifications relevant to the current investigation, specifically the addition of magnesium, are detailed here. This study utilized a 240 V electric melting furnace to heat a 250-g mass of as-received material, which was 99.65% pure magnesium, until the temperature reached 650 °C. The molten alloy will be retained in the graphite crucible for 10 minutes to ensure the uniform temperature distribution and complete homogenisation cycle. The melt was stirred for 30 seconds to promote effective mixing between the base Al-Si alloy and the added

magnesium. This step was crucial in achieving a homogeneous distribution of magnesium within the molten alloy. All other experimental process conditions and experiment setup were maintained as in previous work to facilitate a direct comparison [37], [38]. Figure 2 illustrates the schematic diagram depicting the process involved in the DTM experimental works.

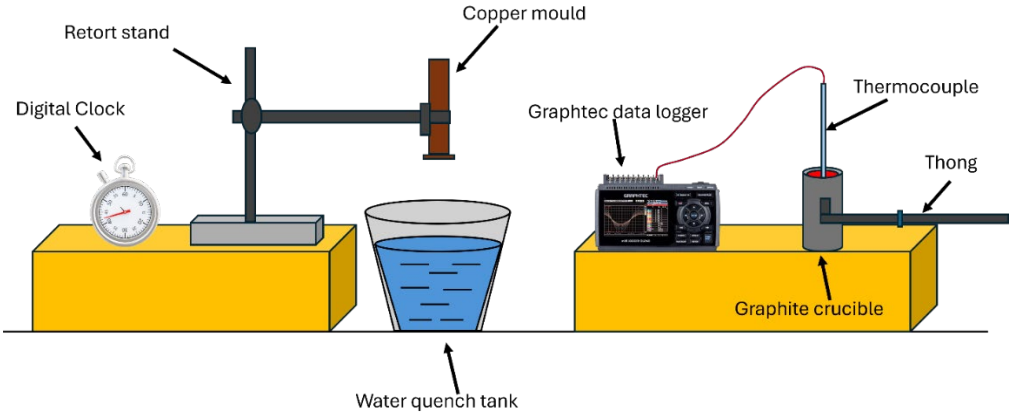

Figure 2: The DTM experimental setup to produce SSM feedstock billets.

2.3 Mechanical Properties Sample Preparation

The density of the feedstock billets was determined using the buoyancy and displacement techniques, both of which are based on Archimedes' principle. Density measurements are crucial in evaluating the porosity of the feedstock billets, as variations in density can indicate the presence of internal voids or inconsistencies within the material structure. The weight of each feedstock billet was measured using a mass balance before it was submerged in water. The water level readings inside the beaker, taken before and after the feedstock billets were immersed in water, were recorded. In this study, the density of each feedstock billet was calculated using Archimedes' principle as expressed in Eq 3

$$\rho fb = \frac{Wfb \ x \ \rho H_20}{W \ H_20} \qquad Eq\ 3$$

Where the density (ρ_{fb}) is expressed in g/cm³, the mass of the feedstock billet (W_{fb}) was measured in grams, while the density of water (ρ_{H2O}) was taken as 1 g/cm³. The mass of the DTM feedstock billets when fully submerged in water (W_{H2O}) was recorded in ml. The density values obtained indicate the porosity level within the feedstock billets. The density value obtained from the literature was 2.70 g/cm³ [25], [39]. A measured average density exceeding 2.70 g/cm³ suggests a lower porosity content, indicating a more compact and defect-free structure. Conversely, billets

with an average density below 2.70 g/cm³ exhibit higher porosity, which can potentially affect their mechanical properties and overall integrity.

The circular DTM feedstock billet samples were prepared in accordance with the ASTM E8 standard. The fractography of the selected samples was analysed using a JSM-IT200 Scanning Electron Microscope to examine fracture mechanisms and failure modes. The Vickers hardness test was conducted using a Vickers hardness testing machine, following the ASTM E384 standard. Before testing, the samples were meticulously ground using abrasive paper to ensure a clean, flat surface for accurate indentation measurements. Special attention was given to the placement of indentation points, as indentations near or within pores could distort the hardness readings and compromise the reliability of the results.

3. Results and Discussion

3.1 Mechanical Properties

3.1.3 Density Measurement

The average density and porosity measurements of DTM feedstock billets are presented in Table 4. The density values measured in these experimental works were slightly higher than the density of aluminium alloy reported in the literature, which is generally 2.7 g/cm^3 [25], [39]. The density obtained from the experimental work was compared with values reported in the literature. An average density greater than 2.7 g/cm³ indicated lower porosity, while samples with density values below 2.7 g/cm³ exhibited higher porosity levels.

Table 4 Average density and porosity measurements of DTM feedstock billets with and without magnesium addition.

Run	Pouring temperature (°C)	Holding time (s)	Magnesium addition (wt.%)	Density (g/cm^3)	Porosity level
1	590	10	1	2.65	Low
2	630	10	1	2.64	Low
3	590	20	1	2.62	Moderate
4	630	20	1	2.61	Moderate
5	590	15	0.5	2.58	Moderate
6	630	15	0.5	2.55	High
7	590	15	1.5	2.7	Lowest
8	630	15	1.5	2.69	Low
9	610	10	0.5	2.59	Moderate
10	610	20	0.5	2.54	High
11	610	10	1.5	2.68	Low
12	610	20	1.5	2.67	Low
13	610	15	1	2.62	Moderate
14	610	15	1	2.61	Moderate
15	610	15	1	2.6	Moderate
16	590	20	-	2.53	Highest

The results showed that sample 7, with a pouring temperature of 590 °C, a holding time of 15 s, and 1.5 wt.% magnesium, had the highest density value at 2.7 g/cm³. Meanwhile, the samples without magnesium addition,

produced at a pouring temperature of 590 °C and a holding time of 20 s, had the lowest density value of 2.53 g/cm³. It was apparent that sample 7 had the lowest porosity level compared to the other samples. The density results correlate with those of a previous study, which showed that adding magnesium to the alloy improved its properties [40], [41]. The variation in density values can be attributed to the formation of porosity that arises during solidification as molten metal shrinks, creating pores. Additionally, the entrapment of hydrogen gas within the molten metal further contributes to the formation of pores [42]. Hydrogen gas becomes concentrated in the liquid near the solid-liquid interface during dendrite growth. The hydrogen gas, which migrates from the interdendritic zone, may not have sufficient time to escape from the mould, resulting in large porosity within the samples.

3.1.3 Ultimate Tensile Strength & Vickers Hardness

The ultimate tensile strength (UTS), yield strength (YS), elongation, and Vickers hardness results were presented in *Table 5*. It was apparent that the mechanical properties of DTM feedstock billets exhibited significant variations with changes in processing parameters. The results clearly show that sample 7, with a pouring temperature of 590 °C, a holding time of 15 s, and a magnesium addition of 1.5 wt.%, has the highest UTS, YS, and Vickers hardness value at 147 MPa, 113 MPa, and 137 HV, respectively. Meanwhile, sample 16, without magnesium addition, has the lowest mechanical properties, with a UTS, YS, and Vickers hardness value of 44 MPa, 36 MPa, and 73 HV, respectively.

Table 5: Value of UTS, YS, elongation and Vickers hardness for DTM feedstock billets.

Sample	Pouring Temperature (°C)	Holding Time (s)	Magnesium Addition (wt.%)	UTS (MPa)	Ys (MPa)	Elongation (%)	Vickers Hardness (HV)
1	590	10	1	110	83	0.87	121
2	630	10	1	46	32	0.6	98
3	590	20	1	108	107	1.13	119
4	630	20	1	62.	55	1.6	116
5	590	15	0.5	65	57	1.5	116
6	630	15	0.5	77	75	1.23	118
7	590	15	1.5	147	113	0.4	137
8	630	15	1.5	133	109	0.43	128
9	610	10	0.5	95	89	1.17	119
10	610	20	0.5	97	84	1.17	119
11	610	10	1.5	131	92	0.53	126
12	610	20	1.5	111	91	0.57	122
13	610	15	1	55	38	0.67	112
14	610	15	1	69	65	0.8	116
15	610	15	1	67	60	0.7	116
Without magnesium addition	590	20	-	44	36	1.5	73

The addition of magnesium increased, resulting in a reduction of elongation to fracture in the DTM feedstock billets. The decrease in elongation to fracture is due to increased formation of Mg_2Si and changes in the intermetallic compounds that develop in the alloys with rising Mg content [32], [33], [43]. The decrease in elongation to fracture of the DTM feedstock billets correlated directly with an increase in Mg content due to the formation of brittle phases like Mg2Si, π-Al9FeMg3Si5, and Q-Al5Cu2Mg3Si5, which are linked to the Mg content in the alloys [32], [44].

The areas where significant differences have been found between the DTM samples with magnesium addition and the DTM samples without magnesium addition. The results align with previous studies, which indicate that the addition of magnesium to aluminium alloys enhances their mechanical properties [33], [41], [43]. The addition of 1.5 wt.% magnesium contributed to the formation of intermetallic phases in the alloy, thereby enhancing its mechanical properties. The alloy's mechanical properties are improved due to the changes in the morphology of the α-Al during the DTM process. The mechanical properties results correlated with the density measurement, where higher magnesium content enhanced the properties of the alloy. In addition, the precipitation of intermetallic compounds, which was formed as finely dispersed particles, and the spheroidisation of the eutectic Si particles significantly affect the alloy's mechanical properties [45], [46], [47]. The formation of an intermetallic phase, such as Mg_2Si, significantly enhances the mechanical properties by reducing dislocation movement and refining the grain structure. The refinement of eutectic Si, solid solution strengthening of α-Al, and the presence of the intermetallic phase further enhanced the hardness value by restricting plastic deformation and increasing resistance to indentation.

3.1.3 Fractography

Fractography analysis was conducted to compare the fracture surfaces and provide insights into the failure modes of samples 7, which exhibited the highest mechanical properties, and sample 2, which exhibited the lowest mechanical properties. Figure 3 presents the fracture surface of sample 7, while Figure 4 depicts the fracture surface of sample 2. Based on the fracture surface, it was apparent that both samples exhibited a ductile fracture mode. The formation of dimples in both samples confirms their ductile fracture behaviour [46], [48].

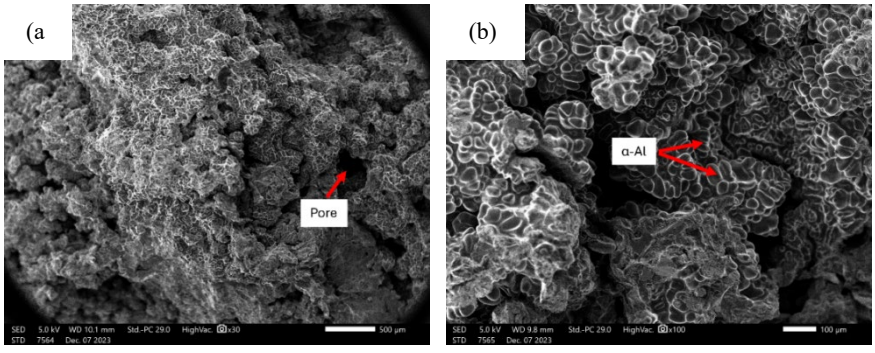

(c)

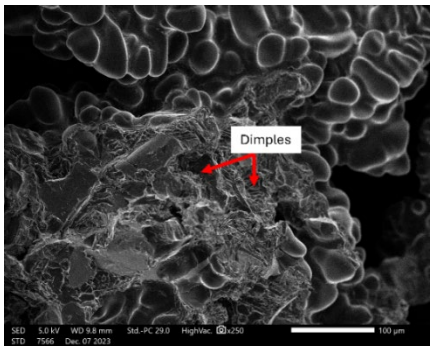

Figure 3: SEM images for tensile fracture surface of sample 7 with (a) 30 x magnification power, (b) 100x magnification power and, (c) 250x magnification power.

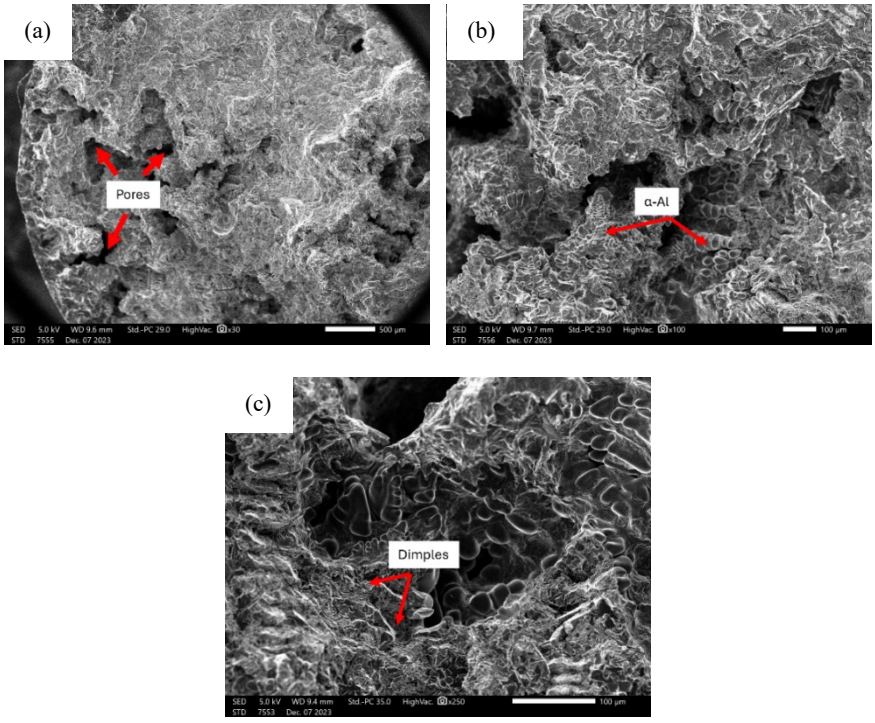

Figure 4: SEM images for tensile fracture surface of sample 2 with (a) 30x magnification power, (b) 100x magnification power, and (c) 250x magnification power.

This dimple fracture surface was formed due to the coalescence of microvoids [41]. This occurs because the Si particles and intermetallic Mg_2Si precipitates exhibit different deformation rates compared to the α-Al matrix. As the materials undergo tensile stress, these differences lead to the initiation and growth of microvoids, ultimately contributing to the formation of fractures. The incorporation of magnesium into the alloy modified the surface morphology of the aluminium alloy, leading to the formation of an intermetallic phase due to the reaction between Al and Mg. An increasing percentage of magnesium addition resulted in enhanced intermetallic phase formation. Additionally, the formation of pores has a significant impact on the mechanical properties of sample 2. These pores can be attributed to casting defects resulting from degassing procedures performed during the casting process. The tensile testing of the sample resulted in the stress being applied, causing small pores to expand into large cracks, which

led to fracture as these cracks continued to propagate. These factors consequently resulted in the alloy's reduced mechanical properties. Pores typically form during solidification as the molten metal contracts. The presence of hydrogen gas trapped within the molten metal also plays a role in the development of pores [42]. The reduction in mechanical properties of the samples is a result of pore formation caused by gas entrapment and shrinkage porosity. The characteristics of materials produced by SSM processing were found to be enhanced primarily due to a reduction in porosity.

3.2 Response Surface Methodology (RSM) Analysis

The response surface methodology (RSM) is a set of mathematical and statistical analysis techniques that are beneficial for studying and modelling problems where multiple factors influence a key variable and can be examined. A three-dimensional graph was plotted to represent the relationship between pouring temperature, holding time, and magnesium addition. The optimal parameters were more easily determined in three-dimensional plots than in two-dimensional plots.

3.2.1 Graphical Analysis for Density Measurement

The three-dimensional surface plots for density measurement are depicted in Figure *5* to Figure *7*, illustrating the functional relationship between the processing parameters and density measurement. In these graphs, term A represents the pouring temperature, B denotes the holding time, and C corresponds to the amount of magnesium added. The three-dimensional graph revealed that adding magnesium to the alloy increases the density value of the DTM feedstock billets. The results further predict that a higher amount of magnesium addition leads to a higher density result.

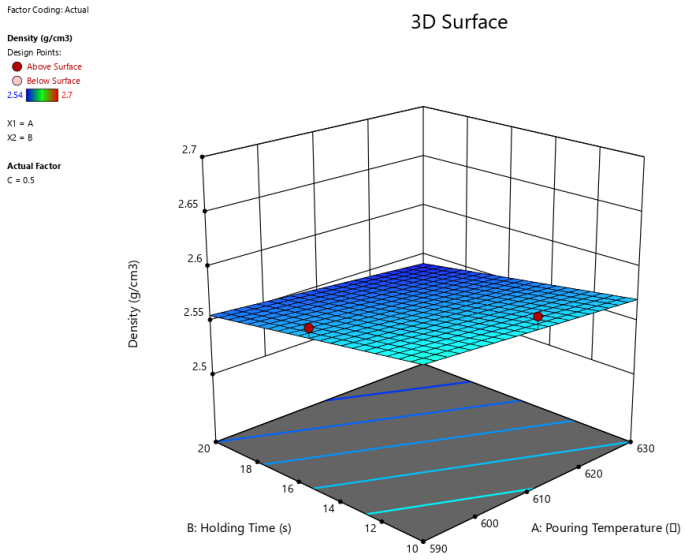

Figure 5: Three-dimensional density measurement graph for DTM feedstock billet mechanical properties with 0.5 wt.% magnesium addition.

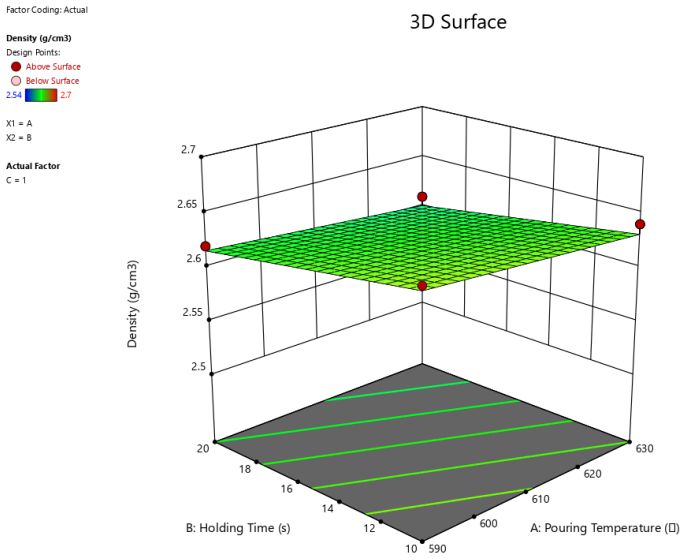

Figure 6:Three-dimensional density measurement graph for DTM feedstock billet mechanical properties with 1 wt.% magnesium addition.

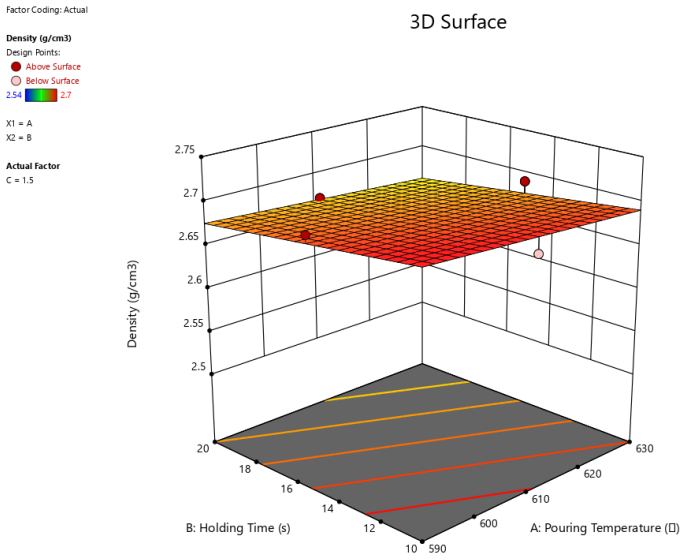

Figure 7: Three-dimensional density measurement graph for DTM feedstock billet mechanical properties with 1.5 wt.% magnesium addition.

Figure *5* illustrates that with 0.5 wt.% magnesium, the density ranges from 2.54 g/cm³ to 2.59 g/cm³. Similarly, Figure *6* shows that for 1 wt.% magnesium, the density value ranges from 2.61 g/cm³ to 2.65 g/cm³. Meanwhile, Figure *7* presents the response surface for a 1.5 wt.% magnesium addition, where the density value falls between 2.66 g/cm³ and 2.71 g/cm³. The three-dimensional surface plot illustrates the relationship between pouring temperature, holding time, and magnesium addition on the density value of the DTM feedstock billet. Adding 0.5

wt.% magnesium, the highest recorded density was 2.59 g/cm³ at a pouring temperature of 590 °C and a holding time of 10 seconds. Similarly, for 1 wt.% magnesium, the maximum density of 2.65 g/cm³ was achieved under identical conditions. The highest density, 2.71 g/cm³, was observed at a 1.5 wt.% magnesium addition with a pouring temperature of 590 °C and a holding time of 10 seconds.

3.2.2 Ultimate Tensile Strength

Figure 8 to Figure 10 illustrate the three-dimensional surface plot for UTS, plotted against pouring temperature, holding time, and magnesium addition. In Figure 8, the predicted grain diameter ranges from a minimum of 54 MPa to a maximum of 82 MPa. The smallest UTS value of 54 MPa is observed in samples processed at 630 °C, with a holding time of 10 s and 0.5 wt.% magnesium addition. Conversely, the largest UTS value of 82 MPa is recorded at the lowest pouring temperature and longer holding time.

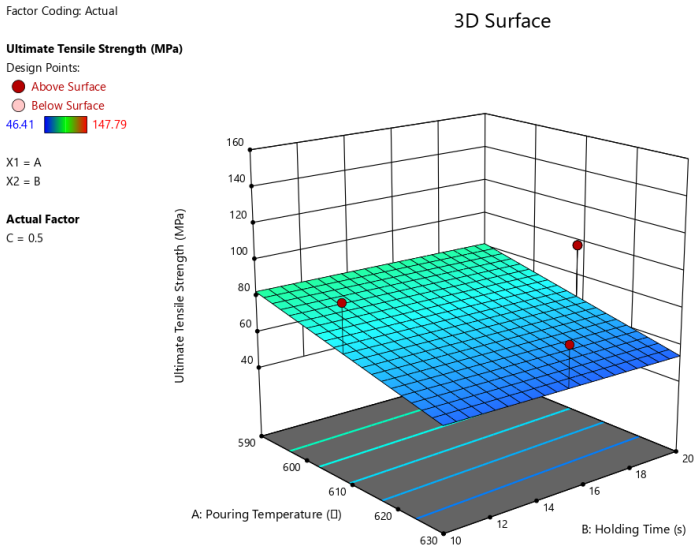

Figure 8: Three-dimensional UTS graph for DTM feedstock billet mechanical properties with 0.5 wt.% magnesium addition.

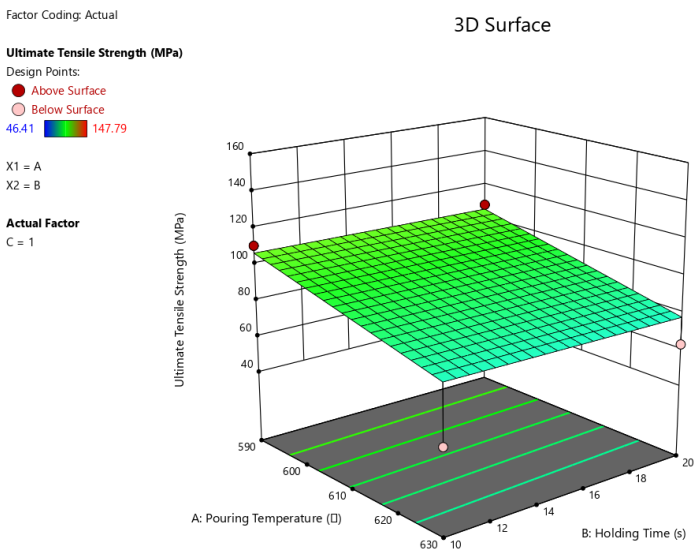

Figure 9: Three-dimensional UTS graph for DTM feedstock billet mechanical properties with 1 wt.% magnesium addition.

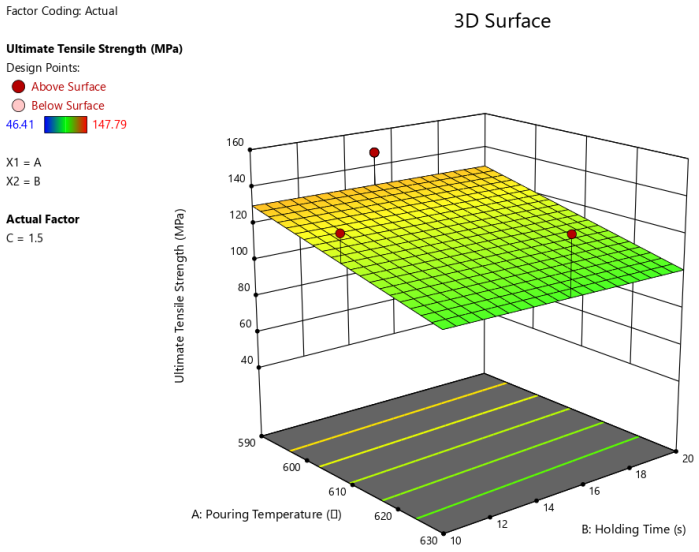

Figure 10: Three-dimensional UTS graph for DTM feedstock billet mechanical properties with 1.5 wt.% magnesium addition.

Similarly, Figure 9 shows that with 1 wt.% magnesium addition, the UTS values vary from 78 MPa to 106 MPa. The smallest UTS value of 78 MPa was achieved at higher pouring temperatures and shorter holding times. In contrast, the maximum UTS value of 106 MPa occurs at lower pouring temperatures and longer holding times. Figure 10 presents the three-dimensional plot for 1.5 wt.% magnesium addition, with the UTS values ranging from 101.57 MPa to 129.65 MPa. The smallest UTS value of 101 MPa is observed at the highest pouring temperature and shortest holding time, while the highest UTS value of 129 MPa is recorded in samples processed at 590 °C with a holding time of 20 s.

3.2.3 Vickers Hardness

Figure 11 to Figure 13 present the three-dimensional surface plots for Vickers hardness, showing values ranging between 98 HV and 137 HV for the 15 DTM samples. The addition of magnesium significantly affects the mechanical properties of DTM feedstock billets. In Figure 11, where magnesium addition is 0.5 wt.%, the lowest Vickers hardness value of 104 HV occurs at higher pouring temperatures and longer holding times. In contrast, the highest Vickers hardness value of 122 HV was recorded at a pouring temperature of 590°C and a holding time of 10 s. Additionally, Figure 12 displays the three-dimensional circularity graph for the addition of 1 wt.% magnesium. From the graph, the Vickers hardness values range from 110 HV to 128 HV. Figure 13 presents the Vickers hardness graph for 1.5 wt.% magnesium addition, indicating that the minimum Vickers hardness value of 115 HV is observed at higher pouring temperatures and longer holding times. In contrast, the maximum Vickers hardness value of 134 HV is recorded at lower pouring temperatures and shorter holding times.

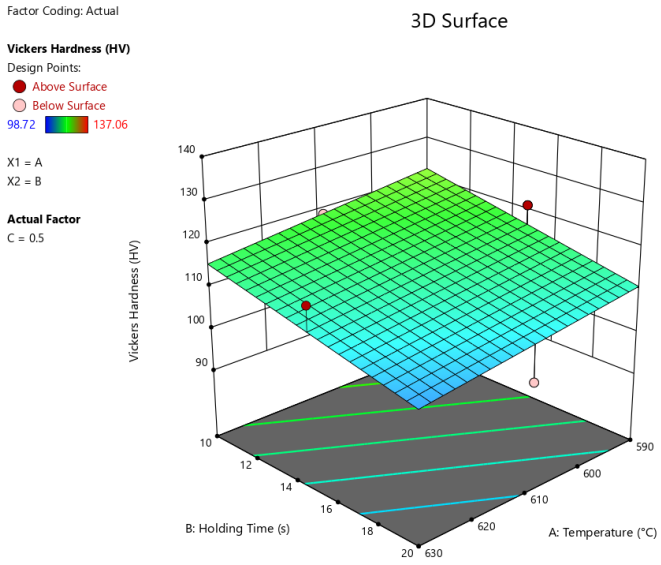

Figure 11: Three-dimensional Vickers hardness graph for DTM feedstock billet mechanical properties with 0.5 wt.% magnesium addition.

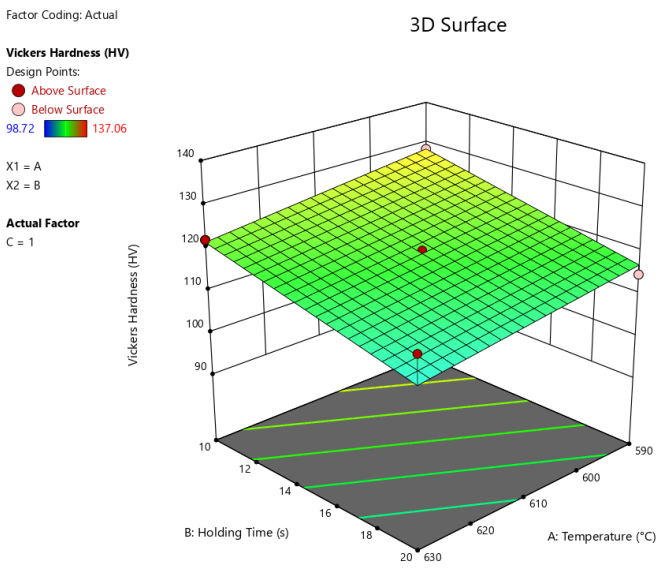

Figure 12: Three-dimensional Vickers hardness graph for DTM feedstock billet mechanical properties with 1 wt.% magnesium addition.

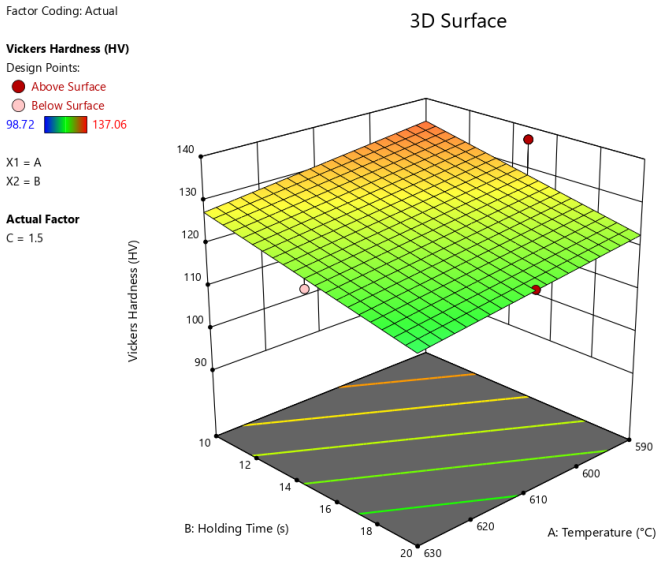

Figure 13: Three-dimensional Vickers hardness graph for DTM feedstock billet mechanical properties with 1.5 wt.% magnesium addition.

3.3 BBD Model Analysis

The three-level matrix generated by BBD with the response obtained experimentally for the density, ultimate tensile strength and hardness of the DTM feedstock billets. Total 15 experiment runs were designed by BBD as in Table 3 with the independent variable consist of pouring temperature X_1 (590°C, 610°C and 630°C), holding time X_2 (10s, 15s and 20 s) and magnesium addition X_3 (0.5 wt.%, 1 wt.% and 1.5 wt.%). The influence of the process parameters on density ($Y_{Density}$), ultimate tensile strength (Y_{UTS}), and Vickers hardness (Y_{HV}) was modeled using first- and second-order polynomial coefficients. The corresponding response equations (Eq. 4, Eq. 5, and Eq. 6) were

formulated from coded data obtained through Design Expert 13 software. The density and UTS are represented by a first-order linear polynomial model, while the Vickers hardness are characterized by second-order quadratic polynomial models.

I. Density:

$$Y_{Density} = 2.77708 - 0.000375X_1 - 0.003X_2 + 0.12\,X_3 \quad \text{Eq 4}$$

II. UTS

$$Y_{UTS} = 467.6011 - 0.0901X_1 - 0.1073X_2 + 47.0725X_3 \quad \text{Eq 5}$$

III. Vickers hardness

$$Y_{HV} = 703.31 - 0.93X_1 - 29.33X_2 - 61.44X_3 + 0.05X_1X_2 + 35.63X_3^2 \quad \text{Eq 6}$$

In Eqs. 4, 5, and 6, a positive sign signifies a synergistic effect of the factors, whereas a negative sign signifies an antagonistic effect of the factors [49]. This equation was employed to forecast the response of each factor under the specified conditions. The equation determines the relative influence of the factors by comparing the coefficients of each factor.

3.4 Analysis of variance (ANOVA)

The analysis of variance (ANOVA) was carried out for the density, UTS and Vickers hardness response were given in Table 6. The ANOVA was achieved to determine the important interaction effects of factors that influence the response efficiency. The F-value serves as an indicator of the extent of variance between the means in relation to the variability present within each individual sample. The threshold for the significance level of the P-value is typically established at a value lower than 0.05. If the null hypothesis is true, the results obtained would be expected to occur by chance at 0.05 or lower error rate.

Table 6 ANOVA results for density, UTS and Vickers hardness for the DTM feedstock billets.

Source	**Density ($Y_{Density}$)**	**UTS (Y_{UTS})**	**Vickers Hardness (Y_{HV})**
Model	Linear	Linear	Quadratic
Standard Deviation	0.01	26.59	5.02
Mean	2.62	92.09	119.38
Coefficient of variation (%)	0.49	28.87	4.2
R^2	0.94	0.43	0.76
Adjusted R^2	0.92	0.27	0.63
Predicted R^2	0.89	0.03	0.13

Adeq Precision	22.1993	5.4392	8.9208
F-Value	60.45	2.81	5.83
P-Value	<0.0001	0.0889	0.0113

I. ANOVA of Density

A linear model was employed to analyse the density measurement. The sufficiency of the models was corroborated through a rigorous analysis of the statistical characteristics, which encompass R^2, adjusted R^2, and adequate precision. The model F-value of 60.45 implies the model is significant. There is only a 0.01 % chance that an F-value this large could occur due to noise. In ANOVA, a high F-value suggests greater variation between samples relative to the variation within samples. The adequacy precision ratio density of 22.20, which indicate an adequate signal. A ratio of adequacy precision greater than 4 is desirable for the response. Figure 14 illustrates the predicted versus actual plot for the density measurement calculated from the model. The observed values closely align with the regression model, demonstrating a strong agreement between the predicted and actual values.

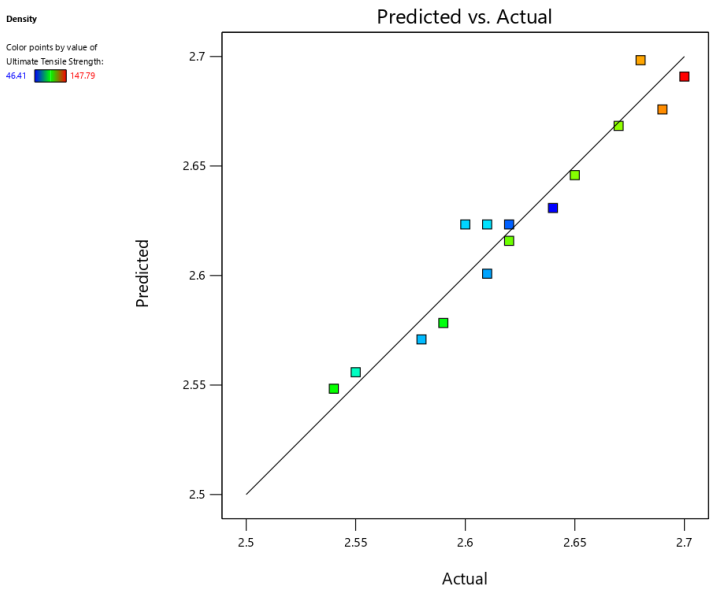

Figure 14 Predicted against actual plot for density measurement.

II. ANOVA of UTS

The ANOVA of UTS indicates that the linear model type. The model's F-value of 2.81, with a p-value of 0.0889, is insignificant, with only an 8.89 % probability that such a large F-value could occur due to noise. The adjusted R^2 value was 43.38 %, respectively. However, the negative value of the predicted R^2 of 3.64 % shows that the overall mean may better predict the response than the current model. Additionally, the model demonstrated an

adequate precision value of 5.4392. Figure 15 shows the predicted against actual plot for UTS value, where the observed values closely align with the regression model, demonstrating a strong agreement between the predicted and actual values. The porosity within the DTM feedstock billets causes significant variability in tensile strength test results, resulting in inconsistent trend patterns. Consequently, the statistical model faces difficulty in identifying a substantial correlation between input factors and tensile properties, resulting in an insignificant p-value in the ANOVA table. A negative predicted R^2 value suggests that the model's predictive capabilities are limited by the high variability in tensile strength resulting from the presence of porosity. The porosity formation causes mechanical properties to vary, challenging the model to identify consistent patterns. As a result, the model's predictive accuracy is less reliable.

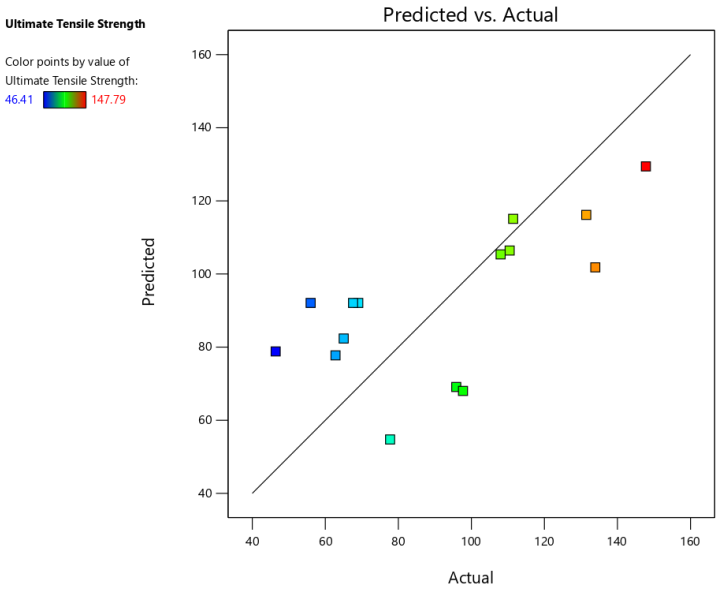

Figure 15 Predicted against actual plot for UTS value**.**

III. ANOVA of Vickers hardness

The ANOVA of Vickers hardness indicates that the response using quadratic model. The model's F-value of 5.83 and p-value of 0.0113 indicate statistical significance. The probability of obtaining such an F-value due to noise is only 1.13 %. The adjusted R^2 and predicted R^2 values were 63.29 % and 13.26 %, respectively. The Predicted R^2 of 0.1321 is not as close to the Adjusted R^2 of 0.6329 as one might normally expect since, the difference is more than 0.2. This may indicate a large block effect to the model. The adequacy precision Vickers hardness ratio of 8.92 indicates an adequate signal where this model can be used to navigate the design space. The comparison between observed and predicted values is further depicted in Figure 16.

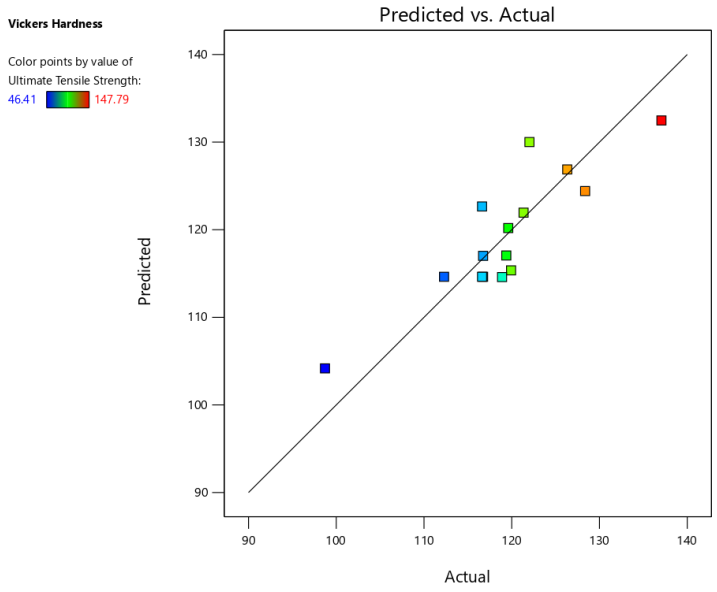

Figure 16 Predicted against actual plot for Vickers hardness.

4. Conclusion

The combination of processing parameters has a significant effect on the mechanical properties of the Al-Si alloy with magnesium addition. The average density value of DTM feedstock billets ranges from 2.53 g/cm^3 to 2.7 g/cm^3. The results showed that sample 7, with a pouring temperature of 590 °C and a holding time of 15 s, containing 1.5 wt.% magnesium, had the highest density value at 2.7 g/cm³. Meanwhile, the samples without magnesium addition, produced at a pouring temperature of 590 °C and a holding time of 20 s, had the lowest density value of 2.53 g/cm³. Additionally, sample 7 exhibits the highest ultimate tensile strength (UTS) value at 147 MPa. Meanwhile, the sample without magnesium, produced at 590 °C with a holding time of 20 s, has the lowest UTS value of 44 MPa. Notably, samples with magnesium addition consistently show higher UTS and Ys compared to those without magnesium addition. The Vickers hardness test value ranged between 73 HV and 137 HV. Sample 7 has the highest Vickers hardness value compared to the sample without magnesium addition, which produced the lowest hardness value at 73 HV. It was apparent that the sample with magnesium addition had a higher mechanical property than the sample without magnesium addition. RSM has explored the optimal combination of pouring temperature, holding time, and magnesium addition to produce Al-Si alloy semi-solid feedstock billets with the desired mechanical properties, as produced via DTM. The three-dimensional surface plots were developed to establish a relationship between the DTM experimental variables and the response. Results from RSM indicated that incorporating magnesium up to 1.5 wt.% was predicted to yield optimal DTM feedstock billets with improved mechanical characteristics. The findings suggest that employing response surface methodology, specifically the Box-Behnken approach, is a highly effective method for identifying the optimal parameters that maximize the mechanical properties of DTM feedstock billets.

Acknowledgements

The authors would like to thank Universiti Malaysia Pahang, Al-Sultan Abdullah, for funding this work with the International Publication Grant, Project Number RDU 243301.

Author contribution: The manuscript was written by Muhammad Faez Bin Mohamad Tajudin. The manuscript was supervised by Dr Asnul Hadi Bin Ahmad, Dr Juliawati Binti Alias, Dr Mohd Rashidi Bin Maarof and Dr Sumsun Naher.

Funding: The authors would like to thank Universiti Malaysia Pahang, Al-Sultan Abdullah, for funding this work with the International Publication Grant, Project Number RDU 243301.

Availability of data and material: Data can be made available upon request, subject to the approval of all parties involved in the research.

Consent for publication: The participants provided informed consent for the publication of their statements. All authors voluntarily agree to participate in this research study.

Conflict of Interest: The authors declare that they have no known competing financial interests or personal relationships that could have appeared to influence the work reported in this paper.

References

[1] Z. Lang *et al.*, "Study on Semi-solid Slurry Preparation Process, Microstructure, and Mechanical Properties of Truck Bracket," *International Journal of Metalcasting*, Jan. 2024, doi: 10.1007/s40962-024-01330-8.

[2] Y. Zhang, Y. Shan, X. Liu, and T. He, "An integrated multi-objective topology optimization method for automobile wheels made of lightweight materials," *Structural and Multidisciplinary Optimization*, vol. 64, no. 3, pp. 1585–1605, Sep. 2021, doi: 10.1007/s00158-021-02913-3.

[3] L. Huang, X. Du, Q. Zhuang, C. Huang, and J. Li, "Effect of Alloying Elements Mg and Cu on the Modification of Eutectic Silicon in Hypoeutectic Al–Si Alloys," *Metals (Basel)*, vol. 13, no. 12, 2023, doi: 10.3390/met13121995.

[4] M. Y. Khalid, R. Umer, and K. A. Khan, "Review of recent trends and developments in aluminium 7075 alloy and its metal matrix composites (MMCs) for aircraft applications," *Results in Engineering*, vol. 20, no. March, p. 101372, 2023, doi: 10.1016/j.rineng.2023.101372.

[5] X. You *et al.*, "A review of research on aluminum alloy materials in structural engineering," *Developments in the Built Environment*, vol. 17, no. January, p. 100319, 2024, doi: 10.1016/j.dibe.2023.100319.

[6] S. L. Lü, S. Sen Wu, Z. M. Zhu, P. An, and Y. W. Mao, "Effect of semi-solid processing on microstructure and mechanical properties of 5052 aluminum alloy," *Transactions of Nonferrous Metals Society of China (English Edition)*, vol. 20, no. SUPPL. 3, pp. 758–762, 2010, doi: 10.1016/S1003-6326(10)60577-8.

[7] F. Czerwinski, "An overview of thixoforming process," 2017, doi: 10.1088/1757-899X/257/1/012053.

[8] G. Vaneetveld, A. Rassili, J. C. Pierret, and J. Lecomte-Beckers, "Improvement in thixoforging of 7075 aluminium alloys at high solid fraction," *Solid State Phenomena*, vol. 141–143, no. February 2015, pp. 707–712, 2008, doi: 10.4028/www.scientific.net/ssp.141-143.707.

[9] Z. Chang, N. Su, Y. Wu, Q. Lan, L. Peng, and W. Ding, "Semisolid rheoforming of magnesium alloys: A review," Oct. 01, 2020, *Elsevier Ltd*. doi: 10.1016/j.matdes.2020.108990.

[10] J. Jiang, Y. Zhang, Y. Wang, G. Xiao, Y. Liu, and L. Zeng, "Microstructure and mechanical properties of thixoforged complex box-type component of 2A12 aluminum alloy," *Mater Des*, vol. 193, p. 108859, 2020, doi: 10.1016/j.matdes.2020.108859.

[11] M. Rosso, I. Peter, and P. Torino, "New frontiers for thixoforming," *International Journal of Microstructure and Materials Properties*, vol. 8, pp 113-, 2013.

[12] A. Pola, M. Tocci, and P. Kapranos, "Microstructure and properties of semi-solid aluminum alloys: A literature review," *Metals (Basel)*, vol. 8, no. 3, 2018, doi: 10.3390/met8030181.

[13] A. H. Ahmad, S. Naher, and D. Brabazon, "Effects of cooling rates on thermal profiles and microstructure of aluminium 7075," *International Journal of Automotive and Mechanical Engineering*, vol. 9, no. 1, pp.

1685–1694, 2014, doi: 10.15282/ijame.9.2013.18.0140.
[14] R. Mehrabian and M. C. Flemings, “Rheological Behavior of Sn-15 Pct Pb in the Crystallization Range,” vol. 3, no. July, 1972.
[15] M. S. Rao and A. Kumar, “Slope Casting Process: A Review,” in *Casting Processes*, T. R. Vijayaram, Ed., Rijeka: IntechOpen, 2022, ch. 1. doi: 10.5772/intechopen.102742.
[16] D. J. Browne, M. J. Hussey, A. J. Carr, and D. Brabazon, “Direct thermal method: New process for development of globular alloy microstructure,” *International Journal of Cast Metals Research*, vol. 16, no. 4, pp. 418–426, 2003, doi: 10.1080/13640461.2003.11819618.
[17] A. H. Ahmad, S. Naher, and D. Brabazon, “Direct Thermal Method of Aluminium 7075,” *Adv Mat Res*, vol. 939, pp. 400–408, 2014, doi: 10.4028/www.scientific.net/AMR.939.400.
[18] D. Brabazon, D. J. Browne, and A. J. Carr, “Mechanical stir casting of aluminium alloys from the mushy state: process, microstructure and mechanical properties,” vol. 326, pp. 370–381, 2002.
[19] A. H. Ahmad, S. Naher, and D. Brabazon, “Injection Tests and Effect on Microstructure and Properties of Aluminium 7075 Direct Thermal Method Feedstock Billets,” no. May, 2014, doi: 10.4028/www.scientific.net/KEM.611-612.1637.
[20] S. Lee and S. Oh, “Thixoforming characteristics of thermo-mechanically treated AA 6061 alloy for suspension parts of electric vehicles,” vol. 131, pp. 587–593, 2002.
[21] M. Z. Omar and K. Alhawari, “An Overview of Semi-Solid Metal Processing,” *Aust J Basic Appl Sci*, no. February 2015, pp. 369–373, 2014.
[22] B. Benjunior, A. H. Ahmad, and M. M. Rashidi, “Direct thermal method pouring temperature and holding time effect on aluminium alloy 6061 microstructure,” *IOP Conf Ser Mater Sci Eng*, vol. 788, no. 1, 2020, doi: 10.1088/1757-899X/788/1/012017.
[23] O. Lashkari and R. Ghomashchi, “The implication of rheology in semi-solid metal processes : An overview,” vol. 182, pp. 229–240, 2007, doi: 10.1016/j.jmatprotec.2006.08.003.
[24] Ł. Rogal, J. Dutkiewicz, H. V Atkinson, L. Lityńska-Dobrzyńska, T. Czeppe, and M. Modigell, “Characterization of semi-solid processing of aluminium alloy 7075 with Sc and Zr additions,” *Materials Science and Engineering: A*, vol. 580, pp. 362–373, 2013, doi: https://doi.org/10.1016/j.msea.2013.04.078.
[25] N. A. Razak, A. H. Ahmad, and M. M. Rashidi, “Investigation of pouring temperature and holding time for semisolid metal feedstock production,” *IOP Conf Ser Mater Sci Eng*, vol. 257, no. 1, 2017, doi: 10.1088/1757-899X/257/1/012085.
[26] A. Witek-Krowiak, K. Chojnacka, D. Podstawczyk, A. Dawiec, and K. Bubala, “Application of response surface methodology and artificial neural network methods in modelling and optimization of biosorption process,” *Bioresour Technol*, vol. 160, pp. 150–160, 2014, doi: 10.1016/j.biortech.2014.01.021.
[27] N. Ferreira *et al.*, “Application of response surface methodology and box–behnken design for the optimization of mercury removal by Ulva sp.,” *J Hazard Mater*, vol. 445, Mar. 2023, doi: 10.1016/j.jhazmat.2022.130405.
[28] M. Sajid, M. K. Nazal, Ihsanullah, N. Baig, and A. M. Osman, “Removal of heavy metals and organic pollutants from water using dendritic polymers based adsorbents: A critical review,” 2018, *Elsevier B.V.* doi: 10.1016/j.seppur.2017.09.011.
[29] R. G. Guan and D. Tie, “A review on grain refinement of aluminum alloys: Progresses, challenges and prospects,” May 01, 2017, *Chinese Society for Metals*. doi: 10.1007/s40195-017-0565-8.
[30] M. F. M. Tajudin, A. H. Ahmad, J. Alias, N. A. A. Razak, and N. A. Alang, “Grain refinement in semi-solid metal processing: current status and recent development,” Jan. 01, 2023, *Springer Science and Business Media Deutschland GmbH*. doi: 10.1007/s00170-022-10590-9.
[31] D. A. Granger and J. Liu, “The Occurence, Effect, and Control Of Twinned Columnar Growth In Aluminum Alloys,” *JOM*, vol. 35, no. 6, pp. 54–59, 1983, doi: 10.1007/BF03338303.
[32] M. S. Salleh, M. Z. Omar, and J. Syarif, “The effects of Mg addition on the microstructure and mechanical properties of thixoformed Al-5%Si-Cu alloys,” *J Alloys Compd*, vol. 621, pp. 121–130, Feb. 2015, doi: 10.1016/j.jallcom.2014.09.152.
[33] M. S. Salleh, A. A. Rahman, R. I. R. Abdullah, N. Siswanto, and S. Subramonian, “Effect of different Mg content on microstructure and mechanical properties of thixoformed Al-Si-Cu-Mg alloys,” *Jurnal Tribologi*, vol. 32, pp. 16–28, 2022.
[34] K. S. Alhawari, M. Z. Omar, M. J. GhazaliI, M. S. Salleh, and M. N. Mohammed, “Microstructural evolution during semisolid processing of Al–Si–Cu alloy with different Mg contents,” *Transactions of Nonferrous Metals Society of China*, vol. 27, no. 7, pp. 1483–1497, 2017, doi: https://doi.org/10.1016/S1003-6326(17)60169-9.

[35] Y. Zheng, W. Xiao, S. Ge, W. Zhao, S. Hanada, and C. Ma, “Effects of Cu content and Cu/Mg ratio on the microstructure and mechanical properties of Al-Si-Cu-Mg alloys,” *J Alloys Compd*, vol. 649, pp. 291–296, 2015, doi: 10.1016/j.jallcom.2015.07.090.

[36] M. F. Mohamad Tajudin, A. H. Ahmad, J. Alias, N. A. Abd Razak, and S. Naher, “Thermal Profile and Microstructure Analysis of Al-Si with the Magnesium Addition under Different Cooling Conditions,” *International Journal of Metalcasting*, 2024, doi: 10.1007/s40962-024-01388-4.

[37] M. F. M. Tajudin, A. H. Ahmad, and M. M. Rashidi, “Effects of Direct Thermal Method Processing Parameters on Mechanical Properties of Semisolid A6061 Feedstock,” vol. 18, no. 1, pp. 8585–8591, 2021.

[38] M. F. M. Tajudin, A. H. Ahmad, and M. M. Rashidi, “Effects of different processing parameters on the semisolid microstructure of Al6061 produced by a direct thermal method,” *IOP Conf Ser Mater Sci Eng*, vol. 1092, no. 1, p. 012008, 2021, doi: 10.1088/1757-899x/1092/1/012008.

[39] C. Kammer, “Aluminum and Aluminum Alloys,” in *Springer Handbook of Materials Data*, W. Warlimont Hans and Martienssen, Ed., Cham: Springer International Publishing, 2018, pp. 161–197. doi: 10.1007/978-3-319-69743-7_6.

[40] K. Logesh, P. Hariharasakthisudhan, A. Arul Marcel Moshi, B. S. Rajan, and K. Sathickbasha, “Mechanical properties and microstructure of A356 alloy reinforced AlN/MWCNT/graphite/Al composites fabricated by stir casting,” *Mater Res Express*, vol. 7, no. 1, 2020, doi: 10.1088/2053-1591/ab587d.

[41] M. A. M. ARIF, M. Z. OMAR, Z. SAJURI, and M. S. SALLEH, “Effects of Cu and Mg on thixoformability and mechanical properties of aluminium alloy 2014,” *Transactions of Nonferrous Metals Society of China (English Edition)*, vol. 30, no. 2, pp. 275–287, Feb. 2020, doi: 10.1016/S1003-6326(20)65212-8.

[42] S. W. Zhen Xu and S. L. and X. C. , Hongbin Wang , Hua Song, “Effect of Cooling Rate on Microstructure and Properties of Twin-Roll Casting 6061 Aluminum Alloy Sheet,” vol. 3, pp. 1–11, 2020.

[43] M. S. SALLEH, M. Z. OMAR, K. S. ALHAWARI, M. N. MOHAMMED, M. A. M. ALI, and E. MOHAMAD, “Microstructural evolution and mechanical properties of thixoformed A319 alloys containing variable amounts of magnesium,” *Transactions of Nonferrous Metals Society of China (English Edition)*, vol. 26, no. 8, pp. 2029–2042, 2016, doi: 10.1016/S1003-6326(16)64321-2.

[44] E. Rincon, H. F. Lopez, M. M. Cisneros, and H. Mancha, “Temperature effects on the tensile properties of cast and heat treated aluminum alloy A319,” *Materials Science and Engineering: A*, vol. 519, no. 1, pp. 128–140, 2009, doi: https://doi.org/10.1016/j.msea.2009.05.022.

[45] M. Yildirim and D. Özyürek, “The effects of Mg amount on the microstructure and mechanical properties of Al-Si-Mg alloys,” *Mater Des*, vol. 51, pp. 767–774, 2013, doi: 10.1016/j.matdes.2013.04.089.

[46] M. S. Haque, M. Nomani, A. Akter, and I. A. Ovi, “Synergistic effect of Mg addition on the enhancement of the mechanical properties and evaluation of corrosion behaviors in 3.5 wt % NaCl of aluminum alloys,” *Heliyon*, vol. 10, no. 3, Feb. 2024, doi: 10.1016/j.heliyon.2024.e25437.

[47] K. S. Alhawari, M. Z. Omar, S. Samat, and A. M. Aziz, “Effect of magnesium addition consolidated by the thixoforming process on the wear properties of A319 alloy,” *International Journal of Advanced Manufacturing Technology*, vol. 131, no. 7–8, pp. 4327–4344, Apr. 2024, doi: 10.1007/s00170-024-13288-2.

[48] S. Sarker, M. S. Haque, M. S. A. Alvy, and M. M. H. Abir, “The effects of solution heat treatment on the microstructure and hardness of an aluminum-4% copper alloy with added nickel and tin,” *Journal of Alloys and Metallurgical Systems*, vol. 4, Dec. 2023, doi: 10.1016/j.jalmes.2023.100042.

[49] A. S. Abdulhameed, A. K. T. Mohammad, and A. H. Jawad, “Application of response surface methodology for enhanced synthesis of chitosan tripolyphosphate/TiO2 nanocomposite and adsorption of reactive orange 16 dye,” *J Clean Prod*, vol. 232, pp. 43–56, Sep. 2019, doi: 10.1016/j.jclepro.2019.05.291.